Original Article

Downregulation of hsa_circ_0000885 suppressed osteosarcoma metastasis and progression via regulating E2F3 expression and sponging miR-16-5p

Yanfang Li [a], [1], Zhiqing Wu [a], [1], Jianlin Shen [b], *

[a] Department of Pediatric Surgery, Affiliated Hospital of Putian University, #181 Meiyuan East Road, Putian, 351100, Fujian, China
[b] Department of Orthopedics, Affiliated Hospital of Putian University, #999 Dongzhen East Road, Putian, 351100, Fujian, China

ARTICLE INFO

ABSTRACT

Introduction: Accumulating evidence has shown that circular RNAs (circRNAs) have indispensable functions during tumor progression by regulating gene expression. A previous study found that upregulation of hsa_circ_0000885 indicated a poor clinical outcome of osteosarcoma (OS). However, the regulatory mechanism of this process is unclear.
Methods: This investigation aimed to elucidate how hsa_circ_0000885 regulated OSs. The study used RT-qPCR to investigate hsa_circ_0000885 expression in OS cells. We conducted luciferase reporter assays and analyses to confirm the hsa_circ_0000885 downstream target. We transfected OS cells using different vectors and used Transwell migration, colony formation, western blotting, Matrigel invasion, proliferation, in vivo tumorigenesis, and metastasis assays to identify the role of hsa_circ_0000885 in OS.
Results: The results showed that hsa_circ_0000885 expression altered OS cell lines, and that hsa_circ_0000885 downregulation suppressed OS cell proliferation and invasion using in vivo and in vitro experiments. Luciferase reporter assays verified that miR-16-5p and E2F3 were downstream targets of hsa_circ_0000885. E2F3 overexpression or miR-16-5p inhibition reversed OS cell invasion and proliferation after silencing hsa_circ_0000885. Furthermore, hsa_circ_0000885 affected cancer stem cell differentiation by regulating miR-16-5p/E2F3.
Conclusions: Overall, the results showed that hsa_circ_0000885 downregulation suppressed OS progression and metastasis via regulating E2F3 expression and sponging miR-16-5p.
© 2022, The Japanese Society for Regenerative Medicine. Production and hosting by Elsevier B.V. This is an open access article under the CC BY-NC-ND license (http://creativecommons.org/licenses/by-nc-nd/4.0/).

1. Introduction

Osteosarcoma (OS), an ordinary primary bone tumor among children, adolescents, and advanced stage patients with metastasis have an unsatisfactory prognosis [1]. The survival of OS patients is poor, in spite of advanced surgical methods integrated with multiple chemotherapies in clinical practice. A large percentage of patients suffer from recurrences because of existing distant metastasis [2]. OS patients might therefore benefit from neo

therapeutics, including small molecule-targeted drugs, although these drugs usually cause serious side effects and clinical trial failures [3,4]. Neo OS therapies, particularly those involving complex gene regulation axes or networks, might therefore be effective.

Circular (Circ)RNA is a newly recognized type of special noncoding RNA molecule, which usually includes endogenous RNA molecules constructed by exon transcripts as well as nonlinear reverse splicing, including circRNA molecules with introns. Most cyclic RNAs are connected covalently with other molecules via a 3′,5′-phosphodiester bond without a polyadenylated tail. Therefore, circRNA is more conservative and stable, when compared with the corresponding linear RNA [5,6]. A previous study suggested that circFAT1 sponged miR-375 to induce Yes-associated protein 1 expression in OS cells [7]. Circular RNA circTADA2A enhances OS metastasis and progression via regulating CREB3 expression and sponging miR-203a-3p [8]. This study also showed that

* Corresponding author.
E-mail addresses: ptliyanfang@163.com (Y. Li), 13799003654@139.com (Z. Wu), shenjianlinchina@126.com (J. Shen).
Peer review under responsibility of the Japanese Society for Regenerative Medicine.
[1] Contributed equally as first authors.

hsa_circ_0000885 was upregulated in OS, which functioned as a candidate prognostic biomarker, indicating poor prognoses of OS patients. Hsa_circ_0000885 has been found to be upregulated in the serum of OS patients, which has been shown to be a potential OS diagnostic biomarker [9]. Because the regulatory mechanism involving hsa_circ_0000885 is unknown, the current study aimed to characterize the regulatory mechanism of hsa_circ_0000885 during OS.

2. Materials & methods

2.1. Ethics statement

Four-week-old BALB/c nude mice (n = 24) weighing 15—20 g (SLARC, Shanghai, China) were used. All animal experiments were approved by the Ethics Committee of Affiliated Hospital of Putian University. All surgery and euthanasia were performed under sodium pentobarbital anesthesia (50 mg/kg) by intraperitoneal injection, and all efforts were made to minimize suffering. All mice were sacrificed by using the CO_2 asphyxia method after experiment (The air displacement rate of CO_2 was 20% of container volume per minute).

2.2. Cell culture

Our team obtained six human OS cell lines (HOS, 143B, MG63, KH-OS, U2OS, and SaoS2) and a normal osteoblast cell line (hFOB1.19) from the American Type Culture Collection (Manassas, VA, USA). We cultivated them in Dulbecco's Modified Eagle's Medium (Gibco, Gaithersburg, MD, USA) with 10% fetal bovine serum (FBS), penicillin (100 units/ml), and streptomycin (100 μg/ml) at 37 °C in a humidified atmosphere of 5% CO_2.

2.3. Bioinformatics prediction

Bioinformatics predicted interacting relationships among miRNA, circRNA, and mRNA using *http://starbase.sysu.edu.cn/*.

2.4. RNA interference or overexpression

We obtained the miR-16-5p inhibitor (the final concentration of siRNA was 20 nM), miR-16-5p mimic (the miRNA mimic was 100 nM, mature miRNA for miR-16-5p was 5′-UAGCAGCAC-GUAAAUAUUGGCG-3′), hsa_circ_0000885 silencing vector (si-circ0000885, the final concentration of siRNA was 1 μg, the siRNA for circ0000885 was 5′-GCCUCUACAACCUGAUGAAUU-3′), and the E2F3 overexpression vector (E2F3, the final concentration was 1 μg, cDNA sequence clone into pcDNA3.1 vector) from RiboBio (Guangzhou, China) to perform transfection using Lipofectamine 2000 (Thermo Fisher Scientific, Waltham, MA, USA).

To further validate the effects of hsa_circ_0000885 in the *in vivo* experiments, a lentiviral-based small hairpin RNA (shRNA) (lentiviral vector: CMV-MCS-GFP-PURO; Novagen) targeting hsa_-circ_0000885 was constructed. GFP detection was performed 72 h after infection into U2OS, and at a green fluorescence >95%, the transfection was considered successful. For *in vivo* metastatic detection, pLVX-Luc2-P2A-AcGFP1-puro lentiviral vector (Novagen) was used for U2OS infection and it generated the luc-U2OS cell line.

2.5. Quantitative real-time polymerase chain reaction (qPCR)

We obtained total RNA from skin tissue, and cells from wounds using TRIzol reagent (Invitrogen, Carlsbad, CA, USA). We synthesized and enhanced cDNA from miRNA and mRNA using a TaqMan miRNA Reverse Transcription kit (Thermo Fisher Scientific) and TaqMan microRNA cDNA Synthesis Kit (Thermo Fisher Scientific), respectively.

And performed qPCR using a TaqMan™ MicroRNA Assay kit (Applied Biosystems, Foster City, CA, USA). We used $2^{-\Delta\Delta CT}$ to detect the fold changes of expression, and *U6* and *GAPDH* were used as internal references. We used the following primers to assay hsa_circ_0000885 expression: forward, 5′-ACTGCCAGAAAGTGTGTCCC-3′ and reverse, 5′-CGGGCCTCGTTTTGAACATC-3′. The *miR-16-5p* primers were the following: forward, 5′-TAGCAGCACGTAAATATTGGCG-3′ and reverse: 5′-TGCGTGTCGTGGAGTC-3′. The *E2F3* primers were forward, 5′-AGAAAGCGGTCATCAGTACCT-3′ and reverse, 5′-TGGACTTCGTAGTG-CAGCTCT-3′; The U6 primers were forward, 5′-CTCGCTTCGGCAG-CACA-3′ and reverse: 5′-AACGCTTCACGAATTTGCGT-3′. The GAPDH primers were forward, 5′-AATGGGCAGCCGTTAGGAAA-3′ and reverse: 5′-TGAAGGGGTCATTGATGGCA-3′.

2.6. Colony formation assay

U2OS and 143B cells with different treatments were used to prepare cell suspensions. We transferred 200 cells to 6-well plates, which were cultured in the cell incubator for 10 days. Cellular shape was observed daily and the culture media was changed every 3 days. Prior to the end of the experiment, we recorded cell images using fluorescence microscopy, and washed cells twice using phosphate-buffered saline (PBS). Giemsa dye (500 μL) was then added to each well for 10—20 min, after which the cells were washed three times with doubly-distilled water and imaged using a digital camera.

2.7. CCK-8 assay

Cells were incubated in 10% CCK-8 solution diluted with normal culture medium at 37 °C, resulting in a color change. The proliferation at days 1, 2, and 3 were measured following transfection by measuring the absorbance at 570 nm using a microplate reader.

2.8. Transwell migration and Matrigel invasion assays

Transwell migration and Matrigel invasion assays utilized Transwell chambers (Corning, Corning, NY, USA) (migration) or Transwell chambers precoated with Matrigel (invasion) following standard protocols (BD Biosciences, Bedford, MA, USA). In brief, 200 μL serum-free medium including 5×10^4 treated cells for the migration assay or 1×10^5 treated cells for the invasion assay were transferred to the upper chambers, followed by transfer of 600 μL of complete medium to the lower chambers. After incubating the cells for 1 day, we recorded representative images using an inverted light microscope (Primovert; Carl Zeiss, Jena, Germany). The invaded and migrated cells were then counted using greater than two random fields of view.

2.9. Tumor sphere formation assay

The harvested U2OS and 143B cells were resuspended as single cells in serum-free medium. Following cell sorting, 200 cells/well in 200 μL of serum-free medium were cultured in 96-well plates (ten wells/group), with media changes every 2 days. We then captured five randomly selected regions for using a camera-equipped microplate reader (Leica, Wetzlar, Germany). Finally, we calculated the percentage of spheres as the sphere numbers/200.

2.10. Dual-luciferase reporter assay

We cloned putative miR-16-5p binding site into the *E2F3* target gene 3′-UTR and hsa_circ_0000885 [wild-type (WT) or mutant (MUT)] into the psi-CHECK (Promega, Madison, WI USA) vector downstream of the firefly luciferase 3′-UTR or hsa_circ_0000885 as the primary luciferase signal with Renilla luciferase as the

normalization signal, which were termed E2F3-Wt/circ-0000885-Wt and E2F3-Mut/circ-0000885-Mut, respectively. The psi-CHECK vector provided the Renilla luciferase signal as normalization to compensate the alternations between the harvested efficiencies and transfections. We used Lipofectamine 2000 (Invitrogen Life Technologies) for transfection into HEK293 cells, and detected Renilla and firefly luciferase activities 1 day after transfection using the Dual-Luciferase Reporter Assay System (Promega, Mannheim, Germany) and a luminometer (Molecular Devices, San Jose, CA, USA). We calculated the relative Renilla luciferase activities following the manufacturers' instructions.

2.11. In vivo experiments

Animal experiments followed established procedures [8]. To validate the OS nude mice models, we injected U2OS cells (1×10^6) with a negative control (NC) or shRNA targeting hsa_circ_0000885 (sh-circ0000885) into the flanks of nude mice, then measured the tumor volumes and weights. N = 6. The Animal Ethics Committee at of The Affiliated Hospital of Putian University approved all animal experiments, and the technicians strictly followed the Guide for the Care and Use of Laboratory Animals (8th edition.).

For tumor metastasis analyses, we stably transfected luminescence-labeled U2OS cells (1×10^5) with the NC. sh-circ0000885 was suspended in sterile PBS and injected into tail vein of 4-week-old nude male mice. After 4 weeks, lung metastasis in vivo was evaluated using a bioluminescence imaging system. Numbers of metastatic foci in lung tissues were calculated according to hematoxylin and eosin staining. N = 6.

2.12. Western blotting

We harvested total protein from cells using a cold radio-immunoprecipitation assay buffer. We used the bicinchoninic acid (BCA) protein assay kit (Pierce Biotechnology, Rockford, IL, USA) to

determine protein concentrations. Protein samples (10 μg) were resolved using 10% SDS-PAGE, transferred a polyvinylidene difluoride membrane, and incubated membranes in primary and secondary antibodies. We obtained antibodies to E2F3, OCT4, Nanog, and glyceraldehyde 3-phosphate dehydrogenase from Abcam (Cambridge, UK).

2.13. Statistical analysis

Data are shown as means ± standard deviation (SD). Statistical analyses were performed using GraphPad Prism (La Jolla, USA) to find significances among groups. P-values ≤ 0.05 were regarded as statistically significant. Two-tailed Student's t-tests were used to determine significant differences between two groups, and one-way ANOVA with post hoc Bonferroni tests were used to determine significant differences among three or more groups.

3. Results

3.1. Downregulation of hsa_circ_0000885 suppressed OS cell proliferation and tumor growth

We first studied hsa_circ_0000885 expression levels in OS cell lines and in the normal osteoblastic cell line, hFOB1.19. RT-qPCR showed significantly increased expressions of hsa_circ_0000885 in the six human OS cell lines, HOS, U2OS, KH-OS, MG63, SaoS2, and 143B, when compared with the normal osteoblast cell line, hFOB1.19. U2OS and 143B cells had higher hsa_circ_0000885 expression levels; therefore, we selected them the next phase of the study (Fig. 1A). We then constructed siRNA against hsa_circ_0000885 and transfected it into U2OS and 143B cells. RT-qPCR showed that the hsa_circ_0000885 expression levels significantly decreased in U2OS and 143B cells, when compared with the positive control and NC (Fig. 1B). CCK8 (Fig. 1C and D) and the colony formation assays (Fig. 1E and F) validated that hsa_circ_0000885
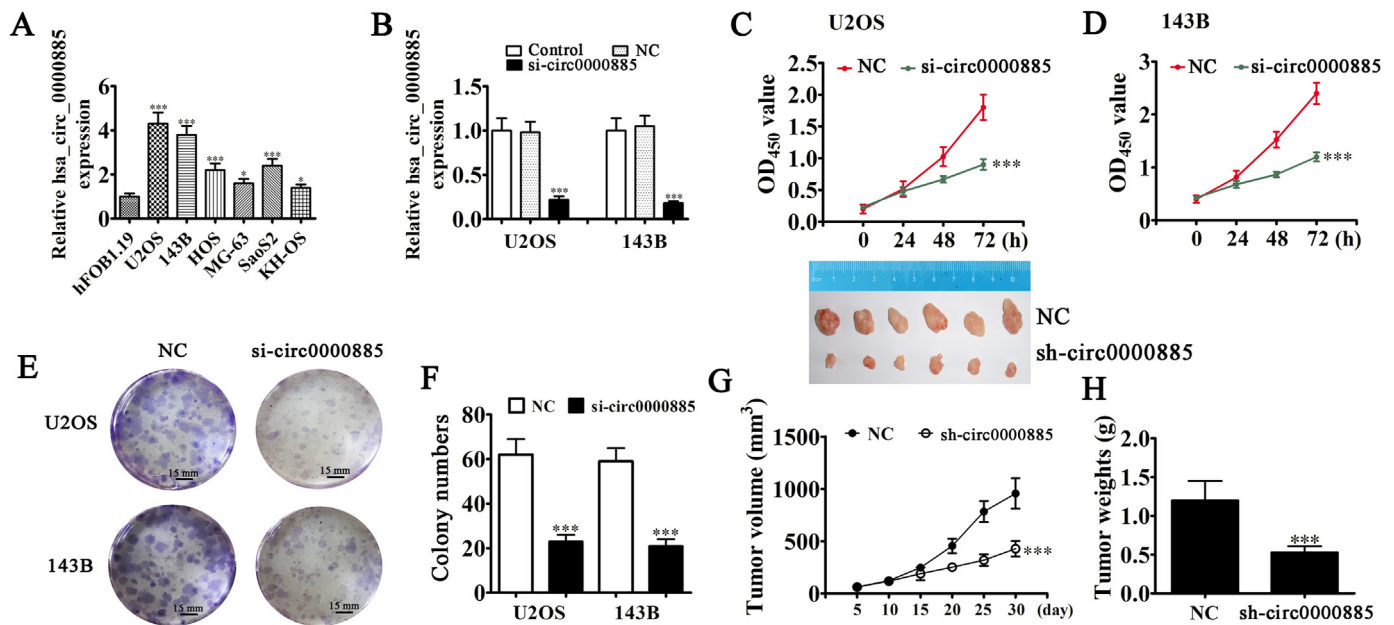
Fig. 1. Downregulation of hsa_circ_0000885 suppressed OS cell proliferation and tumor growth. (A) RT-qPCR shows the expression of hsa_circ_0000885 in OS cell lines and one normal osteoblastic cell line, hFOB1.19. The data are presented as the mean ± SD. *P < 0.05, ***P < 0.001 vs. hFOB1.19. (B) RT-qPCR detection showing the expression of hsa_circ_0000885 in U2OS and 143B cells after transfection with siRNA against hsa_circ_0000885 (si-circ0000885) or negative control (NC). The data are expressed as the mean ± SD. *P < 0.05, ***P < 0.001 vs. the NC. (C and D) The CCK-8 assays showing the proliferation ability of U2OS (C) and 143B (D) cells. The data are expressed as the mean ± SD. ***P < 0.001 vs. the NC. (E and F) Colony formation assays showing the clone numbers of U2OS and 143B cells. The data are expressed as the mean ± SD. ***P < 0.001 vs. the NC. Scale bar, 15 mm. (G and H) The xenograft mice assay in vivo showing the tumor volume (G) and weight (H) of nude mice injected with U2OS cells transfected with sh-circ0000885 or the NC. The data are expressed as the mean ± SD. ***P < 0.001 vs. the NC. N = 6.

silencing suppressed proliferation of U2OS and 143B cells. In the *in vivo* xenograft mice assay, tumor volume (Fig. 1G) and weight (Fig. 1H) in nude mice injected with U2OS cells were decreased after transfection with sh-circ0000885, suggesting that hsa_circ_0000885 downregulation suppressed OS cell proliferation and tumor growth.

3.2. The downregulation of hsa_circ_0000885 suppressed OS cell invasion

The Transwell assay of invasion and migration showed that hsa_circ_0000885 downregulation suppressed invasion and migration in U2OS and 143B cells (Fig. 2A–C). Live imaging showed that U2OS cells were involved in pulmonary metastasis and that hsa_-circ_0000885 silencing decreased pulmonary metastasis, as assessed by decreased numbers of metastatic foci in lung tissues after hematoxylin and eosin staining (Fig. 2D–G), further suggesting that downregulation of hsa_circ_0000885 suppressed OS cell invasion.

3.3. MiR-16-5p and E2F3 were hsa_circ_0000885 downstream targets

Bioinformatics analyses showed that hsa_circ_0000885 could interact with a series of miRNAs such as miR-516a-5p, miR-497-5p, miR-195-5p, miR-16-5p, miR-15b-5p, miR-424-5p, and miR-483-3p. We therefore constructed a luciferase reporter vector (including the hsa_circ_0000885 sequence), then cotransfected it

with different miRNA mimics into HEK293 cells. The results showed that only miR-16-5p significantly decreased the fluorescence intensity, showing that miR-16-5p was the hsa_circ_0000885 downstream target (Fig. 3A). Use of the luciferase reporter further confirmed that miR-16-5p inhibited luciferase activity in WT cells, but not in MUT cell lines (Fig. 3B and C), showing that miR-16-5p was the hsa_circ_0000885 target.

Bioinformatics analyses indicated that E2F3 was the miR-16-5p downstream target. Because, E2F3 expression were relative to the cancer stem cell differentiation. And miR-16-5p can interacted with both E2F3 and circ_0000885 [10,11]. So we selected E2F3 as the target of miR-16-5p. To verify correlations between E2F3 and miR-16-5p, we inserted MUT or WT 3′-UTR-E2F3 sequences containing miR-16-5p binding sequence into the luciferase reporter vector (Fig. 3D). We then transfected the luciferase reporter vector into HEK293 cells along with or without the miR-16-5p mimic. Luciferase reporter analyses showed that miR-16-5p inhibited luciferase activity in WT cells, but not in MUT cell lines (Fig. 3E), indicating that E2F3 was the miR-16-5p target.

3.4. E2F3 overexpression or inhibition of miR-16-5p reversed OS cell proliferation and invasion after silencing hsa_circ_0000885

RT-qPCR confirmed that hsa_circ_0000885 expression decreased after transfection with hsa_circ_0000885-silenced vector. However, miR16-5p inhibitor treatment or overexpressing E2F3 can not restore hsa_circ_0000885 expression in both U2OS and
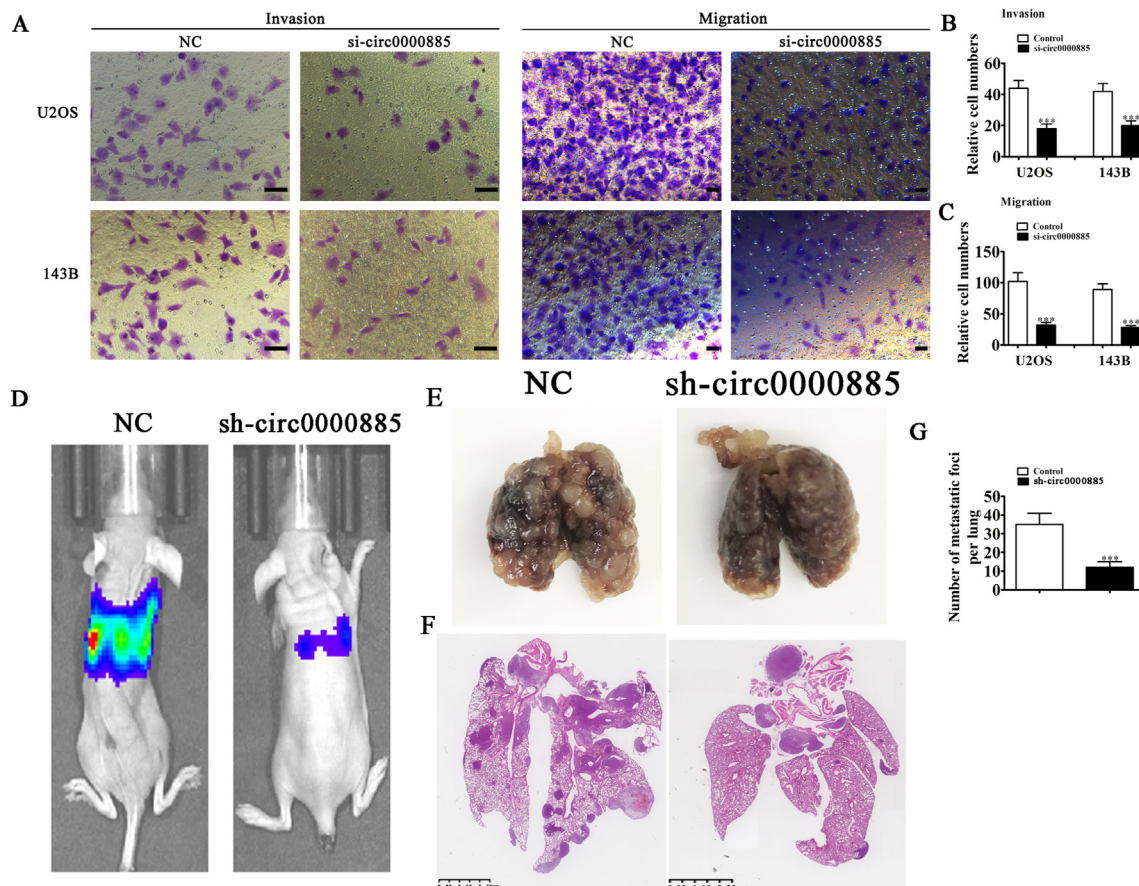
Fig. 2. Downregulation of hsa_circ_0000885 suppressed OS cell invasion. (A–C) Transwell assays showing the migration and invasion assay of U2OS and 143B cells after silencing hsa_circ_0000885. The data are presented as the mean ± SD. ***P < 0.001 vs. the negative control (NC). Scale bar: 100 μm. (D and E) Live imaging showing the metastasis of pulmonary U2OS cells. N = 6. (F and G) The numbers of metastatic foci in lung tissues were calculated according to hematoxylin and eosin staining. The data are expressed as the mean ± SD. ***P < 0.001 vs. the NC. Scale bar: 25 mm.
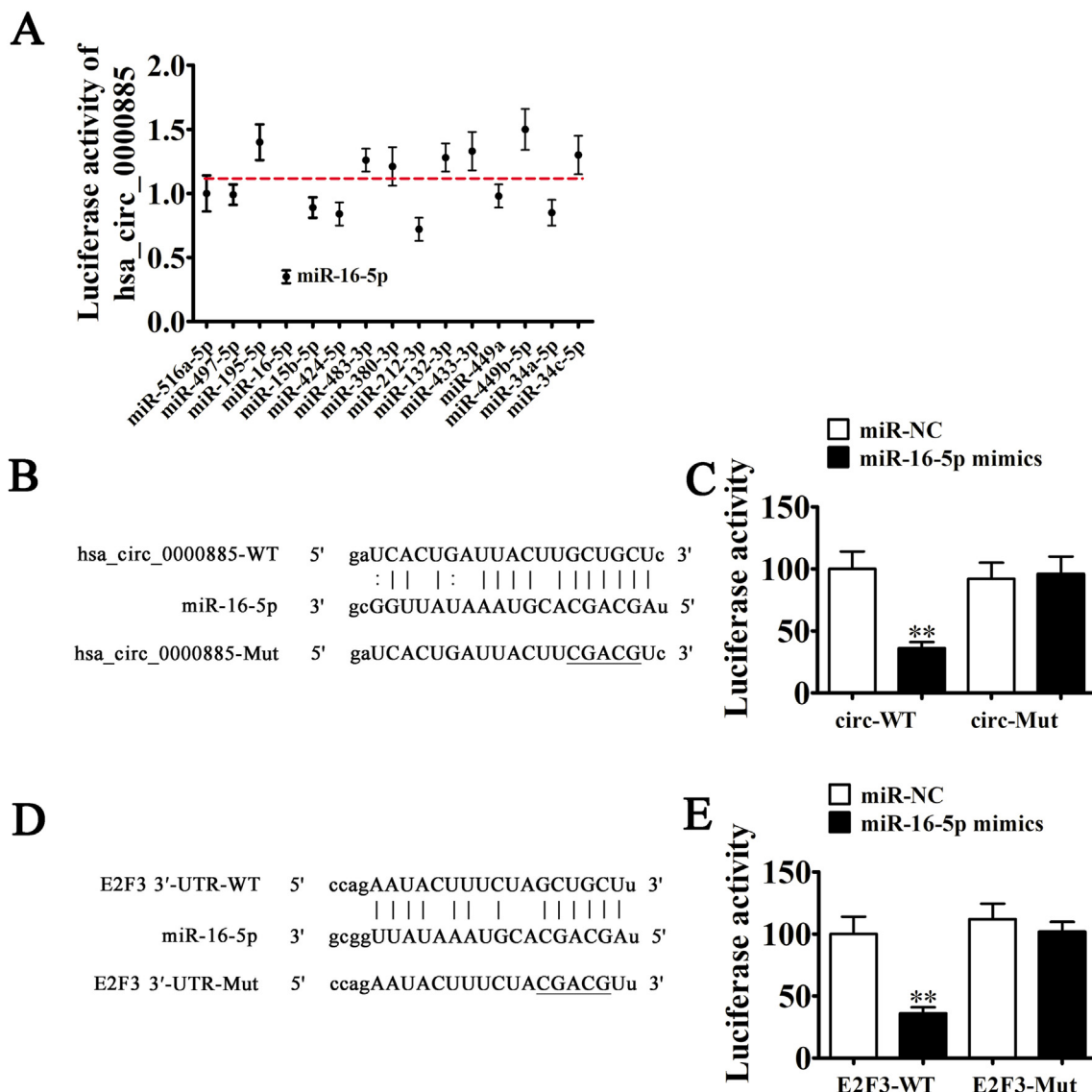
Fig. 3. MiR-16-5p and E2F3 are the downstream targets of hsa_circ_0000885. (A) The luciferase activity of hsa_circ_0000885 in HEK293T cells transfected with different miRNA mimics, which are putative binding sites for the hsa_circ_0000885 sequence. Luciferase activity was normalized using Renilla luciferase activity. (B) The prediction of binding sites of miR-16-5p in hsa_circ_0000885. The mutant (MUT) version of hsa_circ_0000885 is presented. (C) Relative luciferase activity determined 48 h after transfection of HEK293T cells with the miR16-5p mimic/negative control (NC) or hsa_circ_0000885 wild-type (WT)/MUT. Data are presented as the mean ± SD. **P < 0.01. (D) Prediction of binding sites of miR-16-5p within the 3′-UTR of E2F3. The MUT version of 3′-UTR-E2F3 is shown. (E) The relative luciferase activity determined 48 h after transfection of HEK293T cells with miR-16-5p mimic/NC or 3′-UTR-E2F3 WT/MUT. Data are presented as the mean ± SD. **P < 0.01.

143B cells after si-circ0000885 (Fig. 4A and B), suggesting that both miR16-5p and E2F3 were downstream of hsa_circ_0000885. RT-qPCR showed that hsa_circ_0000885 silencing increased miR-16-5p expression. E2F3 overexpression did not reversed si-circ0000885-induced miR-16-5p expression (Fig. 4C and D), indicating that miR-16-5p was downstream of hsa_circ_0000885. The results also suggested that hsa_circ_0000885 silencing decreased E2F3 expression, while inhibition of miR-16-5p reversed E2F3 expression after hsa_circ_0000885 silencing. After transfection with the E2F3 overexpression vector, E2F3 expression significantly increased (Fig. 4E and F), showing that hsa_-circ_0000885 enhanced E2F3 expression by sponging miR-16-5p.

CCK-8 assays demonstrated that E2F3 overexpression or miR-16-5p inhibition reversed OS cell proliferation in both U2OS and 143B cells after silencing hsa_circ_0000885 (Fig. 4G and H). The Transwell assay for invasion and migration detection also showed that E2F3 overexpression or miR-16-5p inhibition reversed OS

cell invasion in both U2OS and 143B cells after silencing hsa_circ_0000885 (Fig. 4I—N).

3.5. Hsa_circ_0000885 influenced cancer stem cell differentiation by regulating miR-16-5p/E2F3

Tumor sphere formation assays in U2OS and 143B cells showed that hsa_circ_0000885 silencing decreased cell division. However, overexpression of E2F3 or inhibition of miR-16-5p recovered the tumor sphere formation abilities (Fig. 5A). Western blot analyses showed that hsa_circ_0000885 silencing decreased expressions of E2F3, OCT4 and Nanog stemness markers of U2OS and 143B cells. However, overexpression of E2F3 or miR-16-5p inhibition recovered expressions of E2F3 and stemness markers OCT4 and Nanog in U2OS and 143B cells (Fig. 5B and C), suggesting that hsa_-circ_0000885 influenced cancer stem cell differentiation by regulation of miR-16-5p/E2F3.
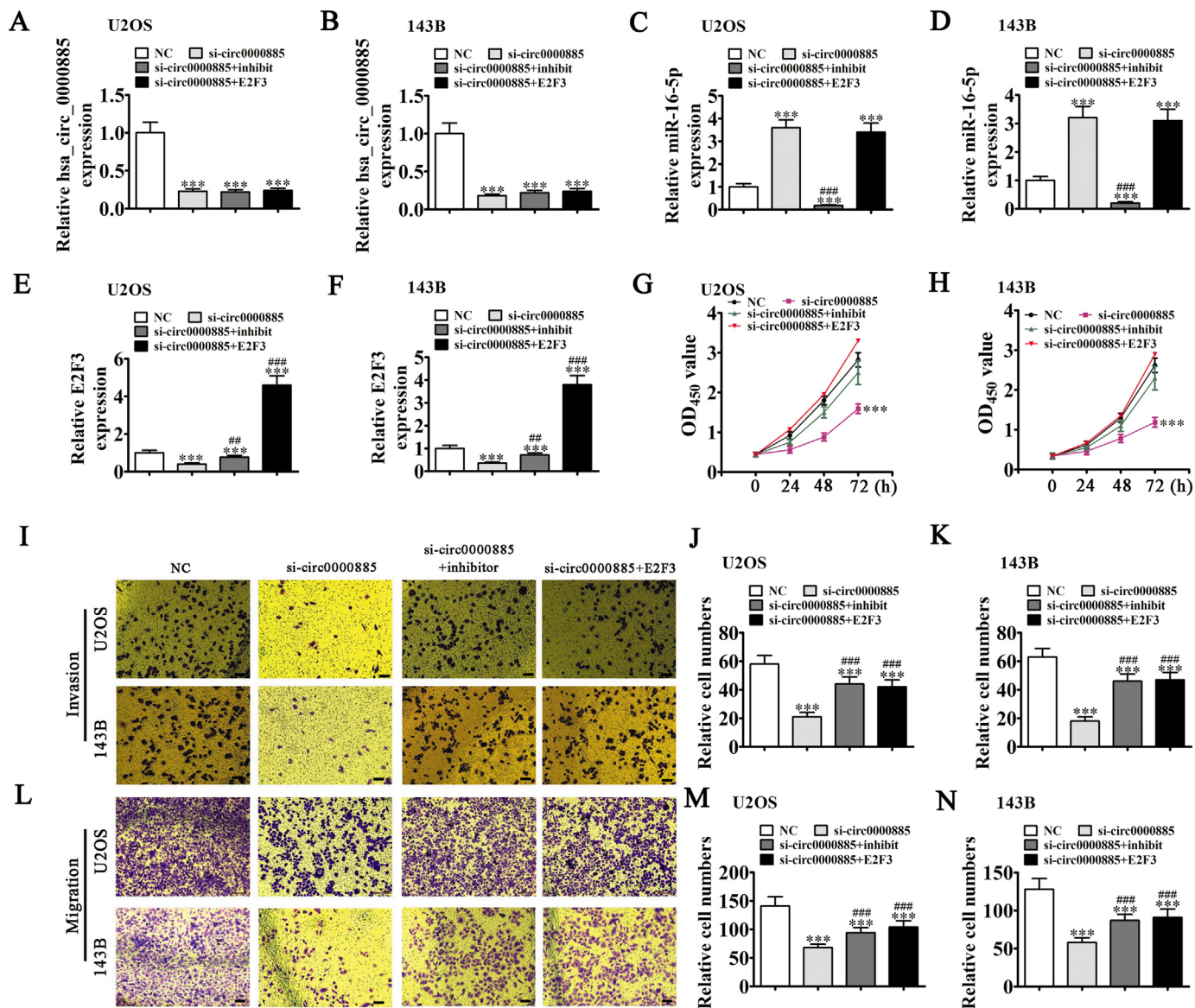
Fig. 4. Overexpression of E2F3 or inhibition of miR-16-5p reversed OS cell proliferation and invasion after silencing hsa_circ_0000885. (A–F) RT-qPCR detection showing the expression of hsa_circ_0000885, miR-16-5p, and E2F3 in U2OS and 143B cells. Data are presented as the mean ± SD; $^{***}P < 0.001$ vs. the negative control (NC); $^{###}P < 0.001$ vs. si-circ0000885. (G and H) CCK8 detection showing the proliferation ability of 143B and U2OS cells. The data are expressed as the mean ± SD. $^{***}P < 0.001$ vs. the NC. (I–N) Transwell assay showing the invasion and migration of U2OS and 143B cells. The data are expressed as the mean ± SD. $^{***}P < 0.001$ vs. the NC. $^{###}P < 0.001$ vs. si-circ0000885. Scale bar: 100 μm.

4. Discussion

CircRNAs comprise part of a family of newly discovered non-coding RNAs. Evidence suggests that circRNAs might be useful as diagnostic markers and therapeutic targets for disparate traits. For example, the circRNA circ-LDLRAD3 is a marker for the diagnosis of pancreatic cancer [12]. The hsa_circ_0013958 is a circRNA, which is a candidate biomarker of lung adenocarcinomas [13], and hsa_circ_0001649 is a candidate biomarker of hepatocellular carcinomas [14]. A previous study found that hsa_-circ_0000885 levels were altered in OS patient tissues and serum, which might function as a prognostic biomarker for the prognoses of OS patients [9]. Recent studies showed that hsa_circ_0000885 expression levels in OS cells were increased when compared with a normal cell line. Hsa_circ_0000885 downregulation suppressed OS cell proliferation and invasion both *in vivo* and *in vitro*, suggesting that hsa_circ_0000885 played a role in the progression of OS.

CircRNAs have recently been shown to function as miRNA sponges to affect gene expression [15,16]. Recent studies found that hsa_circ_0000885 interacted with miR-16-5p, which was confirmed by luciferase reporter analysis. Downregulation of hsa_circ_0000885 promoted miR-16-5p expression, and miR-16-5p inhibition recovered proliferation and invasion abilities after hsa_circ_0000885 silencing. Previous studies showed that miR-16-5p expression decreased in breast cancer (BC) [17], chordomas [18], hepatocellular carcinomas [19], and OS [20]. The miR-16-5p upregulation suppressed metastasis and proliferation in many cancers including hepatocellular carcinomas [21], BC [22], non-small cell lung cancer [23], and cervical cancers [24].

Further studies have reported that miR-16-5p might interact with the 3′-UTR of E2F3 and suppress E2F3 mRNA levels. Luciferase reporter analyses verified that E2F3 was the miR-16-5p target. MiR-16-5p downregulation recovered E2F3 expression after hsa_-circ_0000885. Overexpression of E2F3 reversed proliferation and invasion after downregulation of hsa_circ_0000885. E2F3 is on
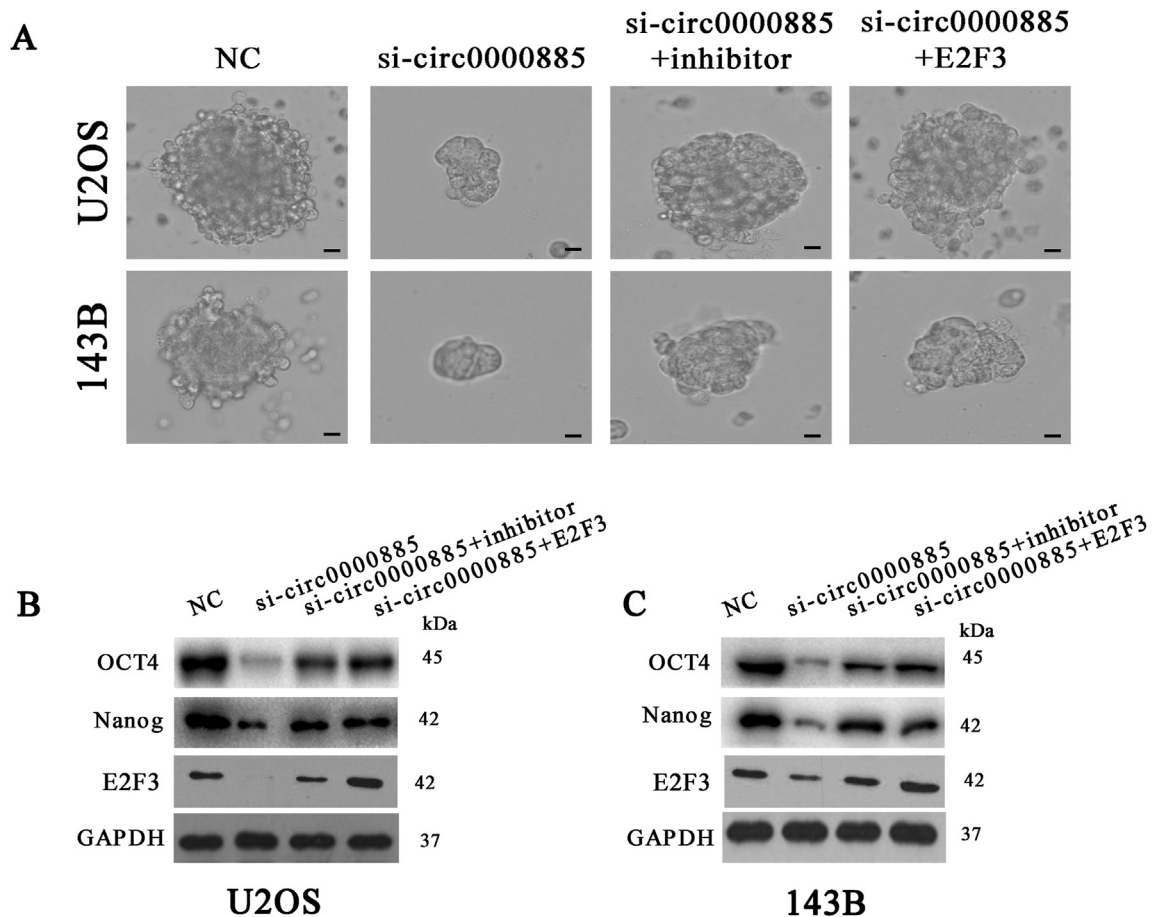
Fig. 5. Hsa_circ_0000885 can influence cancer stem cells differently by regulation of miR-16-5p/E2F3. (A) Images of tumor sphere formation assays of U2OS and 143B cells. Scale bar: 100 μm. (B and C) Western blots showing the expression of stemness markers OCT4, Nanog and E2F3 in U2OS and 143B cells.

chromosome 6p22, which is 91.5 kb long, and E2F3 belongs to the E2F family, which regulates the cell cycle, apoptosis, and proliferation [25]. E2F3 could therefore be used as a marker to predict OS among prostate cancer patients using multivariate analyses [26]. Analyses found that E2F3 regulated cancer stem cell differentiation [27,28]. Cancer stem cells correlate with multiple functions, including cell differentiation, proliferation, migration, and angiogenesis [28]. Inhibiting cancer stem cells can therefore suppress cancer proliferation and invasion. The present study found that hsa_circ_0000885 silencing decreased OCT4 and Nanog stemness marker expressions in U2OS and 143B cells. However, overexpression of E2F3 or miR-16-5p inhibition recovered the OCT4 and Nanog stemness marker expressions in U2OS and 143B cells, suggesting that hsa_circ_0000885 affected cancer stem cell differentiation through the regulation of miR-16-5p/E2F3.

In summary, the present study showed that the downregulation of hsa_circ_0000885 expression decreased OS cell proliferation and invasion by the regulation of miR-16-5p/E2F3 signaling. The results confirmed that hsa_circ_0000885 is a candidate biomarker for diagnostics of OS, and extended the use of drugs to target hsa_circ_0000885, suggesting a possible role of hsa_circ_0000885 in the diagnoses of OS.

Declaration of competing interest

The authors declare that they have no known competing financial interests or personal relationships that could have appeared to influence the work reported in this paper.

Acknowledgements

References

[1] Brown HK, Tellez-Gabriel M, Heymann D. Cancer stem cells in osteosarcoma. Cancer Lett 2017;386:189—95.
[2] Bielack SS, Kempf-Bielack B, Delling G, Exner GU, Flege S, Helmke K, et al. Prognostic factors in high-grade osteosarcoma of the extremities or trunk: an analysis of 1,702 patients treated on neoadjuvant cooperative osteosarcoma study group protocols. J Clin Oncol 2002;20:776—90.
[3] Bishop MW, Janeway KA, Gorlick R. Future directions in the treatment of osteosarcoma. Curr Opin Pediatr 2016;28:26—33.
[4] Otoukesh B, Boddouhi B, Moghtadaei M, Kaghazian P, Kaghazian M. Novel molecular insights and new therapeutic strategies in osteosarcoma. Cancer Cell Int 2018;18:158.
[5] Abdelmohsen K, Panda AC, Munk R, Grammatikakis I, Dudekula DB, De S, et al. Identification of HuR target circular RNAs uncovers suppression of PABPN1 translation by CircPABPN1. RNA Biol 2017;14:361—9.
[6] Sanger HL, Klotz G, Riesner D, Gross HJ, Kleinschmidt AK. Viroids are single-stranded covalently closed circular RNA molecules existing as highly base-paired rod-like structures. Proc Natl Acad Sci USA 1976;73:3852—6.
[7] Liu G, Huang K, Jie Z, Wu Y, Chen J, Chen Z, et al. CircFAT1 sponges miR-375 to promote the expression of Yes-associated protein 1 in osteosarcoma cells. Mol Cancer 2018;17:170.
[8] Wu Y, Xie Z, Chen J, Ni W, Ma Y, Huang K, et al. Circular RNA circTADA2A promotes osteosarcoma progression and metastasis by sponging miR-203a-3p and regulating CREB3 expression. Mol Cancer 2019;18:73.

[9] Zhu K, Niu L, Wang J, Wang Y, Zhou J, Wang F, et al. Circular RNA hsa_circ_0000885 levels are increased in tissue and serum samples from patients with osteosarcoma. Med Sci Monit 2019;25:1499—505.

[10] Gu YH, Shen YC, Ou-Yang Y, Rao XM, Fu DD, Wen FQ. Combined BRM270 and endostatin inhibit relapse of NSCLC while suppressing lung cancer stem cell proliferation induced by endostatin. Mol Ther Oncolytics 2021;22: 565—73.

[11] Pan W, Wu A, Yu H, Yu Q, Zheng B, Yang W, et al. Involvement of the lncRNA AFAP1-AS1/microRNA-195/E2F3 axis in proliferation and migration of enteric neural crest stem cells of Hirschsprung's disease. Exp Physiol 2020;105: 1939—49.

[12] Yang F, Liu DY, Guo JT, Ge N, Zhu P, Liu X, et al. Circular RNA circ-LDLRAD3 as a biomarker in diagnosis of pancreatic cancer. World J Gastroenterol 2017;23: 8345—54.

[13] Zhu X, Wang X, Wei S, Chen Y, Fan X, Han S, et al. hsa_circ_0013958: a circular RNA and potential novel biomarker for lung adenocarcinoma. FEBS J 2017;284:2170—82.

[14] Qin M, Liu G, Huo X, Tao X, Sun X, Ge Z, et al. Hsa_circ_0001649: a circular RNA and potential novel biomarker for hepatocellular carcinoma. Cancer Biomarkers 2016;16:161—9.

[15] Jin J, Chen A, Qiu W, Chen Y, Li Q, Zhou X, et al. Dysregulated circRNA_100876 suppresses proliferation of osteosarcoma cancer cells by targeting microRNA-136. J Cell Biochem 2019;120:15678—87.

[16] Zhang Y, Li J, Wang Y, Jing J. The roles of circular RNAs in osteosarcoma. Med Sci Monit 2019;25:6378—82.

[17] Ruan L, Qian X. MiR-16-5p inhibits breast cancer by reducing AKT3 to restrain NF-kappaB pathway. Biosci Rep 2019;39.

[18] Zhang H, Yang K, Ren T, Huang Y, Tang X, Guo W. miR-16-5p inhibits chordoma cell proliferation, invasion and metastasis by targeting Smad3. Cell Death Dis 2018;9:680.

[19] Cheng B, Ding F, Huang CY, Xiao H, Fei FY, Li J. Role of miR-16-5p in the proliferation and metastasis of hepatocellular carcinoma. Eur Rev Med Pharmacol Sci 2019;23:137—45.

[20] Maximov VV, Akkawi R, Khawaled S, Salah Z, Jaber L, Barhoum A, et al. MiR-16-1-3p and miR-16-2-3p possess strong tumor suppressive and antimetastatic properties in osteosarcoma. Int J Cancer 2019;145: 3052—63.

[21] Liu Z, Wang Y, Wang L, Yao B, Sun L, Liu R, et al. Long non-coding RNA AGAP2-AS1, functioning as a competitive endogenous RNA, upregulates ANXA11 expression by sponging miR-16-5p and promotes proliferation and metastasis in hepatocellular carcinoma. J Exp Clin Cancer Res 2019;38:194.

[22] Haghi M, Taha MF, Javeri A. Suppressive effect of exogenous miR-16 and miR-34a on tumorigenesis of breast cancer cells. J Cell Biochem 2019;120: 13342—53.

[23] Wang Q, Chen Y, Lu H, Wang H, Feng H, Xu J, et al. Quercetin radiosensitizes non-small cell lung cancer cells through the regulation of miR-16-5p/WEE1 axis. IUBMB Life 2020;72:1012—22.

[24] Zhao Z, Ji M, Wang Q, He N, Li Y. miR-16-5p/PDK4-Mediated metabolic reprogramming is involved in chemoresistance of cervical cancer. Mol Ther Oncolytics 2020;17:509—17.

[25] Miles WO, Tschop K, Herr A, Ji JY, Dyson NJ. Pumilio facilitates miRNA regulation of the E2F3 oncogene. Genes Dev 2012;26:356—68.

[26] Bilke S, Schwentner R, Yang F, Kauer M, Jug G, Walker RL, et al. Oncogenic ETS fusions deregulate E2F3 target genes in Ewing sarcoma and prostate cancer. Genome Res 2013;23:1797—809.

[27] Fang Y, Gu X, Li Z, Xiang J, Chen Z. miR-449b inhibits the proliferation of SW1116 colon cancer stem cells through downregulation of CCND1 and E2F3 expression. Oncol Rep 2013;30:399—406.

[28] Bellmunt J. Stem-Like signature predicting disease progression in early stage bladder cancer. The role of E2F3 and SOX4. Biomedicines 2018:6.